geoconvention
Calgary • Canada • May 15-17 2023

Capturing of fine-scaled reservoir heterogeneity through Hyperspectral core scanning

Zach, D, Toews. Patricia, Fraino. John, Gordon. Per, Pedersen.
Department of Geoscience, University of Calgary

Summary

Traditional methods for determining reservoir characteristics rely on logging tools and core analysis; these methods, although effective in many applications, have a low resolution and poor or often non-representative sampling interval ranging from a few centimeters to meters apart. This can be problematic as the resolution and sampling interval of our data can significantly affect how we interpret the reservoir data.

Hyperspectral technology, which has been used in the mining industry for mineralogical characterization, can now, with the introduction of Long Wave Infrared (LWIR), detect tectosilicates. This has significant implications for oil and gas extraction as many plays are in reservoirs composed of tectosilicate minerals (i.e., quartz and feldspar). This now allows for more in-depth characterization of mineralogy and sedimentary fabric at a resolution that was not possible with traditional methods. This research highlights an application of hyperspectral for fine-scaled mineralogical characterization in the Lower Triassic Sulphur Mountain Formation (Montney-equivalent), which could increase production rate predictability and help optimize the frac design for finely laminated reservoirs.

Theory

In unconventional reservoirs, the current methods for understanding reservoir characteristics, such as logging tools and core analysis, can be limited by their low resolution and inadequate sampling intervals. These limitations can affect the interpretation of the data and make it difficult to accurately characterize the reservoir. However, the recent advancements in hyperspectral technology have enabled a more in-depth mineralogical analysis at a resolution that was not attainable before (Alnahwi et al., 2020).

Spectroscopy is the field of study that measures and interprets the electromagnetic spectrum. Each element on the periodic table emits a unique set of wavelengths of light when electrons get excited. Therefore, every element has a unique atomic "fingerprint" that takes the form of a set of wavelengths or a spectrum. Hyperspectral data is like a regular photo in that it has a certain number of bands, each with its own intensity value. A normal image has three bands a red, a green, and a blue. Each band has an intensity value for each pixel, but with hyperspectral images there can be hundreds of bands, each with its own intensity and represents a combination of different elements.

Since hyperspectral images have over 50 times as many bands as regular photos at the mm resolution, to reduce this large data set to something more manageable, each pixel is assigned a class (spectral facies) based on its unique combination of band intensities. Spectral facies are the classification of the rock based on unique spectral characteristics. So instead of having an infinite number of band and intensity combinations, we now have a set number of possible spectral facies.

The spectral facies can then be elementally characterized using traditional methods to acquire elemental composition such as XRF and XRD. Once characterized predictive models (i.e., linear regression and random forest regression) can be built to predict high-resolution elemental data across the entire length of the core.

Methodology

A core was drilled in the Kamenka quarry (Harvie Heights, Alberta, Canada) through Lower Triassic strata of the Sulphur Mountain Formation (Montney-equivalent). The core is ~ 50 m long and was CT scanned, slabbed, and sandblasted at AGAT labs so that a fresh, polished surface could be scanned with Hyperspectral core imaging at Spectrum Geoscience.

Three different Specim© HSI spectrometers were provided by TerraCore and operated by Spectrum Geoscience: i) a high-resolution RGB (120-µm spatial resolution) natural color photograph; ii) two short-wave infrared (SWIR) spectrometers (1.13 mm spatial resolution), which can identify bitumen, water, and clay minerals, and iii), the OWL a high-quality cooled thermal long-wave infrared (LWIR) spectrometer (1.13 mm spatial resolution). The LWIR allows the identification of silicate minerals (quartz and feldspar) that cannot be detected by the SWIR. A list showing the minerals best detected by each spectrometer is shown in Table 1.

Once the Hyperspectral scanning was completed, X-Ray Fluorescence (XRF) was conducted on the core. A total of 437 samples were analyzed every 10 cm along the core length using a Bruker Tracer 5g hand-held X-ray fluorescence spectrometer. The measurement beam size is approximately 3 x 4 mm in area at the nose of the hand-held spectrometer and 31 elements (Na, Mg, Al, Si, P, S, Cl, K, Ca, Ti, V, Cr, Mn, Fe, Co, Ni, Cu, Zn, Ga, As, Se, Rb, Sr, Y, Zr, Nb, Mo, Ba, Pb, Th, U) are reported.

After completing XRF analysis, microhardness was collected at the same locations along the core. A total of 437 samples were analyzed using a Microhardness tool at Spectrum Geosciences Ltd. The measurement was taken every 10 cm in the same locations as the XRF to compare elemental composition and microhardness (mechanical proxy). The measurement area is a circle with a diameter of approximately 3 mm.

Table 1: A list showing the detectability of various minerals by each spectrometer

	Structure	Group	Example	SWIR Response	LWIR Response
Silicates	Inosilicates	Amphibole	Actinolite	Good	Good
		Pyroxene	Diopside	Moderate	Good
	Cyclosilicates	Tourmaline	Dravite	Good	Moderate
	Nesosilicates	Garnet	Andradite	Non-diagnostic	Good
		Olivine	Forsterite	Non-diagnostic	Good
		Zircon	Zircon	Non-diagnostic	Non-diagnostic
	Sorosilicates	Epidote	Clinozoisite	Good	Good
	Phyllosilicates	Mica	Muscovite	Good	Moderate
		Chlorite	Clinochlore	Good	Moderate
		Clay Minerals	Kaolinite	Good	Moderate
			Illite	Good	Moderate
	Tectosilicates	Feldspar	Orthoclase	Non-diagnostic	Good
			Albite	Non-diagnostic	Good
		Silica	Quartz	Non-diagnostic	Good
Non-silicates	Carbonates	Calcite		Good	Good
		Dolomite		Good	Good
	Hydroxides	Gibbsite		Good	Moderate
	Sulphates	Alunite	Alunite	Good	Moderate
			Barite	Non-diagnostic	Good
	Borates		Borax	Good	Uncertian
	Halides	Chlorides	Halite	Moderate	Uncertain
	Phosphates	Apatite	Apatite	Moderate	Good
			Amblygonite	Good	Good
	Hydrocarbons		Bitumen	Good	Uncertain
	Oxides		Haematite	Non-diagnostic	Non-diagnostic
		Spinel	Magnetite	Non-diagnostic	Non-diagnostic
	Sulphides		Pyrite	Non-diagnostic	Non-diagnostic

Courtesy: TerraCore

Additionally, six thin-section samples were prepared by the University of Calgary thin-section prep lab in Calgary, Alberta, Canada. These samples were selected to characterize specific facies identified in the hyperspectral. All samples were impregnated with a blue-dyed epoxy and ground to a standard 30-micron thickness using various grit sizes of silicon carbide powder mixed with water. The samples were stained to identify calcite and carbonate minerals. Samples were observed using a petrographic microscope.

X-Ray diffraction analysis (XRD) was run on six samples from of the same locations as the thin sections. A whole rock analysis was run at Spectrum Geosciences Ltd., on a Rigaku Miniflex XRD. Both whole rock (bulk) and separated clay fraction XRD were run on each sample. The XRD samples were ground to less than a 200 mesh sieve size. A portion of the sample was separated into a less than 2-micron clay fraction. Both air-dried and glycolated clay fractions were run in order to identify swelling clays. Note that XRD analysis results have an approximate +/- 5% error and are considered semi-quantitative data sets. Scanning Electron Microscopy (SEM) was conducted on the same 6 sample locations to characterize the mineralogical fabric of the hyperspectral classes.

Two types of analysis were performed on the data set one was cluster analysis, and the other was regression analysis. The cluster analysis and some of the data cleaning were performed by TerraCore as part of the Hyperspectral data processing. Once the Hyperspectral is scanned, the raw data is sent to a TerraCore processing facility. At the facility, core images were masked to isolate the core from the core boxes. The isolated core images are then depth registered. Once the masking and depth registration was completed, the images were processed into a few different products. These products include Oil and Gas Focused Products, Spectral Features, Spectral Indices, Gridded Features, and various image products. The product used in this research is a variation of the Self Organizing Map (SOM) which is a cluster analysis and a subset of the image products. The Self Organizing Map classification is run for both the SWIR and LWIR spectrometers. The Self Organizing Map is an unsupervised artificial neural network to classify nonlinear data (Kohonen, 1982). The acquired pixels from the slabbed core surface are associated with a SOM class from each spectrometer.

Once the SOM classification is completed, a single vertical column of the data is extracted from the center of the SOM at a resolution of 1 mm. The data is then averaged using a moving window of 4mm so that the data is a representation of what the XRF is seeing. Additional post-processing cleaning involved removing crumbled core bits from the data set and manually correlating each XRF and Hardness data point to the Hyperspectral data. Also, hyperspectral classes that did not correlate to any XRF and Microhardness data point were removed.

The Self Organizing Map classifies the raw reflectance data into 20 SWIR and 20 LWIR classes. The clustering groups the reflectance response of each data point into a class where the data points are more similar to each other than to those in other classes. Once processing and cleaning were completed, each class was elementally and mechanically characterized. Additionally, distribution analysis was conducted on the data set to ensure statistically significant elemental and mechanical differences between the characterized classes. Regression analysis was performed on the hyperspectral class data to evaluate hyperspectrals ability to predict elemental and mechanical properties. Two types of regression were performed, linear regression and random forest regression. The random forest regression model hyperparameters were tuned

using cross-validation. Once the models were trained, the accuracy of the models were tested using an 80/20 train test split on the data. The model was then applied to the entire Hyperspectral dataset.

Results

A total of 40 spectral facies were identified in the core. To relate the spectral facies to the point data acquired from the core (XRF and microhardess) a Random Forest Regression analysis produced better results than a linear regression model. This is in line with findings from another paper which found Random Forest modeling to generate more accurate and precise mineral estimates (Barker et al., 2021). The Random Forest model was used to upscaled the 10 cm XRF sample interval to a sub-centimeter resolution. Figure 1 illustrates the difference in resolution between the XRF and the upscaled elemental data using HSI over the interval 46.75m – 47.75m. The higher resolution of the upscaled data set shows the heterogeneity that is missed with the XRF point sampling. Figure 2 shows a cross plot of the true XRF vs. predicted HSI values over the same 1m interval and has a high correlation (r2 = 0.73). Overall, the hyperspectral scanning can resolve elemental and microhardness data at much higher resolution than traditional methods.

Two unique spectral facies were identified: LWIR facies 7 and 9 which differ from the average properties of the core in both elemental composition and hardness (figure 3). LWIR facies 7 has more Mg and Ca and less Al and K and a higher hardness. LWIR facies 9 has more minor elements (Fe, Mn, Na, Zn, Cl) and less Si and a lower hardness than the average. When we plot the true hardness values of each facies on a histogram, we can clearly see that they are different and not just being skewed by single sample outliers (figure 4). These two spectral facies occur together only in one location in the core and they are separated by a core break.

When mapping the hardness to the spectral facies, we can identify where we have large contrasts in properties between adjacent spectral facies. For example, SWIR 15 and SWIR 9 have a difference in hardness of 45 HLD. Even though we don't have an XRF point exactly on the yellow SWIR 15 spot seen in figure 5 we can use the XRF data from SWIR 15 from other areas to predict the hardness at this specific location then use that to identify fine-scale mechanical heterogeneities.

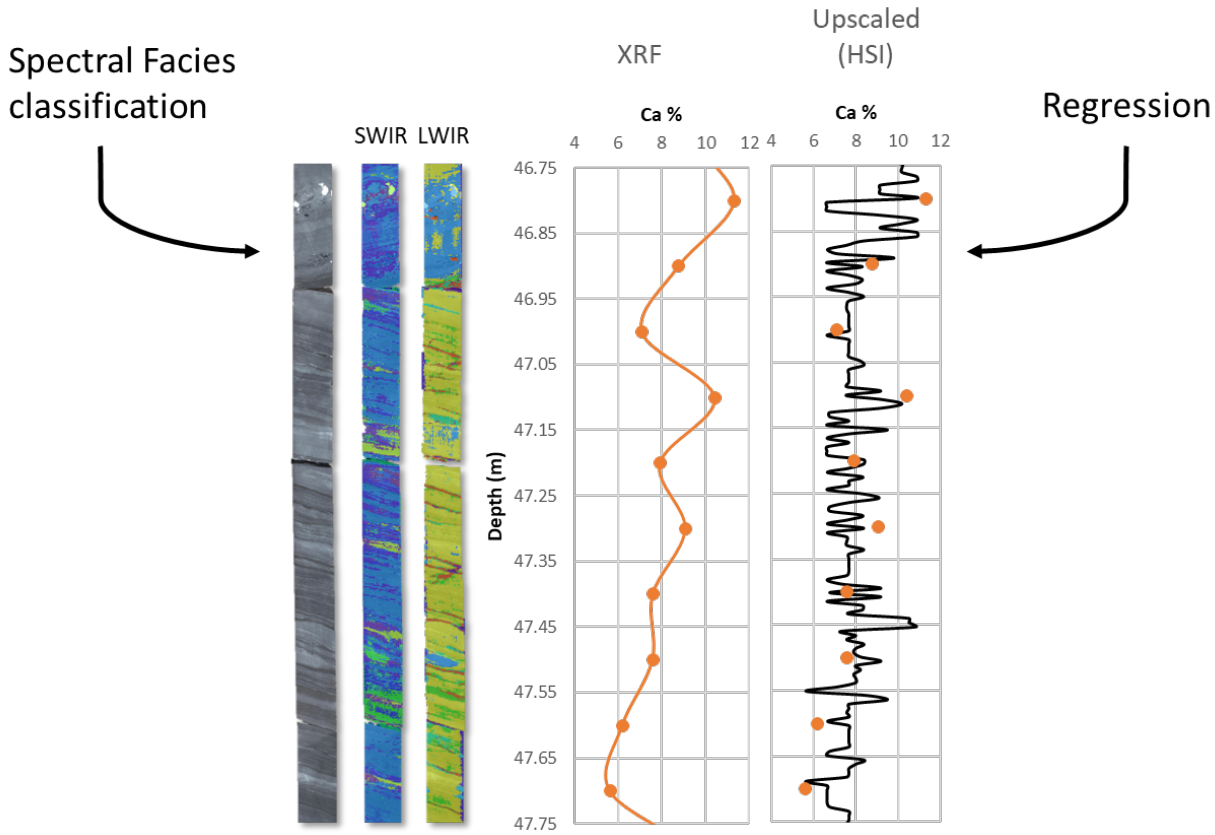

Figure 1: An illustration showing the difference between the spectral facies' classification, the raw XRF values, and the regression analysis. Note the different color hue in the SWIR and LWIR represent different spectral facies.

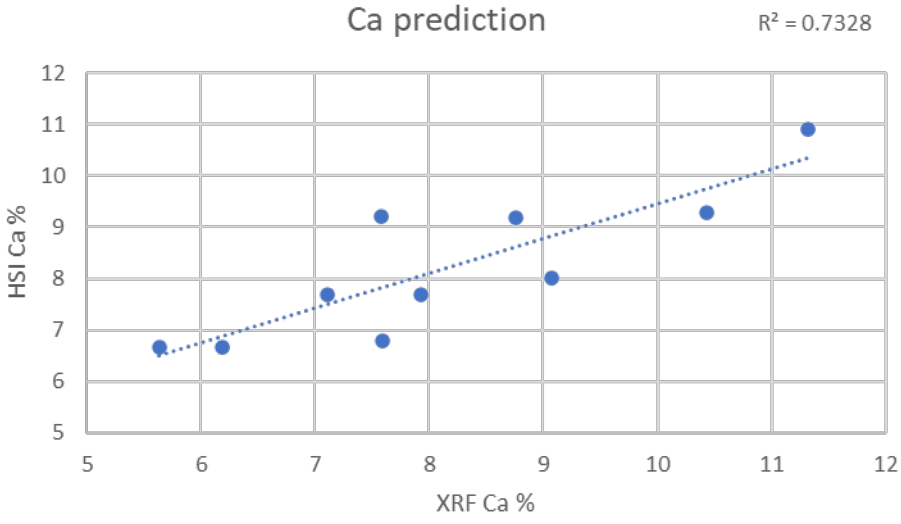

Figure 2: A cross plot of true XRF values (x axis) vs. hyperspectral predicted values (y axis) for Calcium

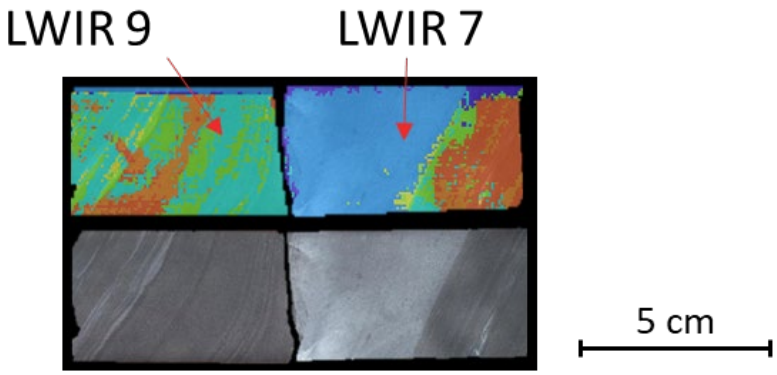

Figure 3: Image of the core showing LWIR 9 facies and LWIR 7 facies with the LWIR class data overlayed onto the core photo

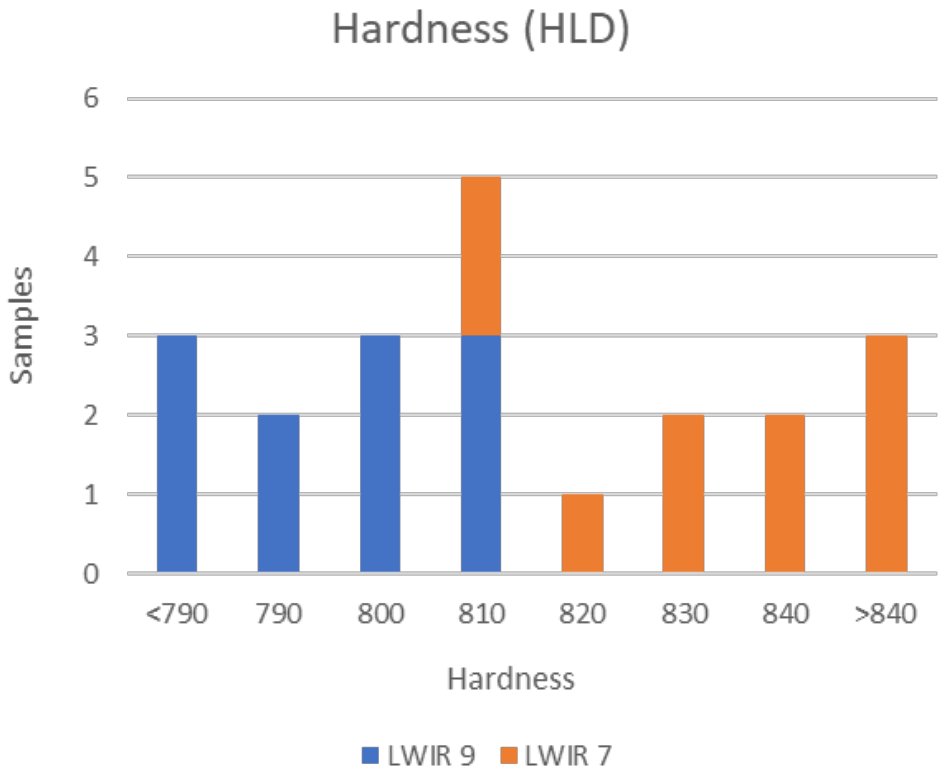

Figure 4: Histogram of the hardness data for LWIR 9 and LWIR 7 showing two statistically different hardness's

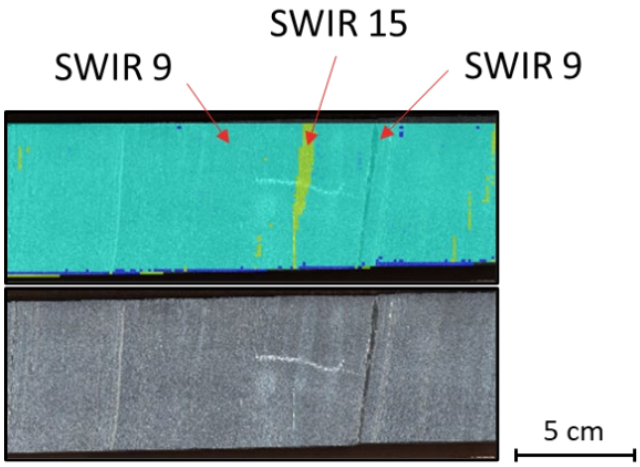

Figure 5: Image of the core showing SWIR 9 facies and SWIR 15 facies with the LWIR class data overlayed onto the core photo.

Conclusions

In conclusion, this paper has presented a new application for hyperspectral scanning technology in the energy industry, specifically for the characterization of fine-grained heterogeneities in sedimentary rock cores. Limitations of traditional methods for determining reservoir characteristics, such as low resolution and unrepresentative sampling intervals, can affect the interpretation of the dataset. Combined Long and Short Wave Infrared hyperspectral technology, can now detect tectosilicates, minerals that are commonly found in oil and gas reservoirs. This capability allows for more in-depth mineralogical characterization at a resolution that is not possible with traditional methods.

The results of this research highlight how the use of hyperspectral scanning technology can improve reservoir understanding, which can help optimize the development design for finely laminated siltstone resources. This technology is expected to evolve further, with more advanced sensors, and a better understanding of the data, to provide even more accurate results in the future.

Additive Information (Implications)

Micro-modeling through the use of digitized core images or FMI logs has been developed to:

- Reduce the uncertainty in upscaling core perm values
- Account for important micro-scale features with high permeability contrasts
- Minimize the effect of sample selection bias

These methods use a binary classification of sand and shale and then assign porosity and perm values to the groups. This is sufficient for when there are interbedded muds and sands, however, some reservoirs are not obviously binary. Hyperspectral would allow for a more in-depth classification using the spectral facies it creates.

Acknowledgments

I would like to thank all of my co-authors. I would also like to thank Louis Kamenka for allowing me to conduct my research and collect samples in his building stone quarry. Thank you to Spectrum Geosciences Ltd. for collecting the SEM, XRF, Hardness, and Hyperspectral data. Thanks to the Global Research Initiative in Sustainable Low Carbon Unconventional Resources (GRI) for funding this project.

References

Alnahwi, A., Kosanke, T., Loucks, R. G., Greene, J., Liu, X., & Linton, P. (2020). High-resolution hyperspectral-based continuous mineralogical and total organic carbon analysis of the eagle ford group and associated formations in south Texas. *AAPG Bulletin*, *104*(7), 1439–1462. https://doi.org/10.1306/02262018156

Barker, R. D., Barker, S. L. L., Cracknell, M. J., Stock, E. D., & Holmes, G. (2021). Quantitative mineral mapping of drill core surfaces II: Long-wave infrared mineral characterization using μXRF and machine learning. *Economic Geology*, *116*(4), 821–836. https://doi.org/10.5382/ECONGEO.4804

Kohonen, T. (1982). Self-organized formation of topologically correct feature maps. *Biological Cybernetics*, *43*(1), 59–69. https://doi.org/10.1007/BF00337288